1-1 (Plenary)

Perspectives in Microscopic Carrier Transport

Tsuneya ANDO

Department of Physics, Tokyo Institute of Technology
2–12–1 Ookayama, Meguro-ku, Tokyo 152-8551, Japan
E-Mail: ando@stat.phys.titech.ac.jp

A brief review is given of recent investigation of transport properties of nanostructures from semiconductor quantum wires and dots to artificial crystals with exotic electronic properties including carbon nanotubes as an example.

I. INTRODUCTION

The development of crystal-growth and lithography technology in last ten years has made it possible to fabricate artificial structures with nano meter size comparable to the wavelength of electrons, excitons etc. and even down to atoms and molecules. Various tools for accurate characterization and observation of such structures have been developed as well as those for precise measurement of their detailed physical properties. In such small-size systems, rich phenomena have been observed, many of which are important also from the point of view of fundamental physics. This in turn offers challenges to fabricate further novel structures. The purpose of this paper is to discuss some examples of recent development and future outlook in the investigation of transport properties of these systems.

II. MESOSCOPIC TRANSPORT

A. Semiconductor Quantum Structure

Mesoscopic structures are fabricated frequently using two-dimensional (2D) systems. A typical 2D system called an inversion layer is realized at a metal-oxide-semiconductor structure, where the integer quantum Hall effect was discovered. A semiconductor superlattice can be fabricated using the crystal growth technique such as molecular beam epitaxy and metal-organic chemical vapor deposition. The motion perpendicular to the interface is quantized and a 2D electron system is realized using the so-called modulation doping in which only the barrier layer is doped with donors. The supreme quality of the heterointerface has made this system ideal and the mean free path can be as large as 100 μm, which made the fractional quantum Hall effect observable.

One important length scale is the Fermi wave length λ_F. When a 2D electron is confined into a wire with width W, for example, the motion perpendicular to the wire is quantized into discrete energy levels and the states consist of one-dimensional (1D) subbands. For an abrupt confinement potential, the energy levels are given by $E_n=(\hbar^2/2m)(\pi n/W)^2$ with $n=1,2,\ldots$. The number of occupied 1D subbands below the Fermi energy, called a channel number, is obtained as $n=[2W/\lambda_F]$. Similar discussion is possible for quantum dots.

In such systems, electrons are confined by an artificial potential and their electron number or density can be almost freely controlled. They are new quantum many-body systems in which both quantum effects and those of mutual interactions are quite strong. A typical example of the manifestation of interactions can be found in the so-called Tomonaga-Luttinger liquid and the Coulomb blockade in quantum dots, dot or antidot lattices, etc.

In macroscopic regimes, the system size is much larger than the phase coherence length, while it is much smaller in microscopic systems. One fundamental and crucial problem on the transport is the crossover from macroscopic to microscopic transport, in particular, the theoretical treatment of phase breaking processes when relevant length scales are all comparable. This problem will not be discussed further in this paper because of the space limitation, however.

B. Ballistic Transport

One most typical example of ballistic transport is the conductance quantization in quantum point contacts in which the conductance changes like a step function with the increase of the gate voltage [1]. Each step with height $e^2/\pi\hbar$ corresponds to the opening up of a new conducting channel. One typical phenomena showing the ballistic electron motion is the so-called magnetic focusing, in which electrons emitted from a quantum point contact are efficiently collected by another point contact onto which electrons are focused following a cyclotron orbit [2]. The ballistic motion manifests itself in quantum wires and crossed wires as a negative bend resistance, a transfer resistance [3], and a quenching and last plateau of the Hall resistivity [4].

C. Quantum Dot and Single-Electron Tunneling

When electrons are trapped into a finite region like quantum dots, the charging energy plays a important role. The Coulomb energy for a dot containing N electrons has a term proportional to $N(N-1)e^2/2$ corresponding to the number of electron pairs interacting with each other. There are positive charges $+Ne$ somewhere which ensure the charge neutrality and the interaction with them leads to a term proportional to N. Therefore, the total energy is given by $E_N=(Q^2/2C)-\alpha eQV_G$, where $Q=-eN$, C is a capacitance, V_G is a gate voltage, and α is a dimensionless constant.

The equilibrium number N of electrons is determined by the conditions $U_N>0$ and $U_{N-1}<0$ with $U_N\equiv E_{N+1}-E_N$. The typical energy required for changing the electron number is given by $(U_N+|U_{N-1}|)/2\sim e^2/C$. The tunnel current across the dot sandwiched by a source and drain electrode through a thin tunnel barrier is generally prohibited at sufficiently low temperatures $k_BT\ll e^2/C$. This is called the Coulomb blockade. At an appropriate gate voltage, ΔU_N vanishes and an electron can tunnel into and out of the dot freely. While the dot contains an extra electron or charge and until the extra charge disappears from the dot, no other electrons can enter

the dot because of the charging energy. Therefore, this tunneling is called a single electron tunneling (SET).

One most typical example of SET devices is a turnstile consisting of a series of two quantum dots [5]. We first apply a certain source-drain voltage in such a way that the tunnel current is prohibited through both quantum dots. When we lower the voltage of the central region between two dots, an electron tunnels into a dot from an electrode but cannot tunnel out to the other electrode because of the Coulomb blockade of another quantum dot. When we raise the voltage, the extra charge $-e$ stored in the central region tunnels out into the other electrode. In this way the charge $-e$ moves from one electrode to other per cycle. The current is determined by e and the frequency of the voltage modulation, which therefore can be used as a current standard.

D. Artificial Atom and Molecule

In a small dot containing just a few electrons, both electron-electron interactions and quantum confinement effects become sufficiently strong to cause a significant modification of the Coulomb oscillation. Such a system can be regarded as an artificial atom [6]. In contrast to the case of a dot containing many electrons the conductance exhibits a Coulomb oscillation as a function of the gate with irregular spacing corresponding to the fact that the addition energy varies sensitively as a function of the number of electrons due to effects of electron-electron interaction and orbital quantization. This behavior can be understood well by a shell filling and Hund's rule analogous to the case of atoms in periodic tables. By combining two or more artificial atoms, artificial molecules can be realized [7]. For a dot with nonzero spin, a singlet coupling with electrons in a surrounding reservoir gives rise to a Kondo effect [8].

III. TOWARD ARTIFICIAL CRYSTAL

A. Quantum-Wire Array

We can impose artificial potential (electrostatic or magnetic) on a 2D electron gas. The potential period can range from the order of 10 Å by using the cleaved edge overgrowth technique to the order of 0.5 μm in systems with a patterned gate. Magnetotransport under a periodic potential shows oscillation arising from the geometrical resonance depending on the commensurability condition between the lattice periodicity and the cyclotron orbit [9]. In a periodic potential electron-electron scattering can contribute to the resistivity through Umklapp processes not conserving the total electron momentum. The resulting T^2 increase of the resistivity was observed [10] and analyzed theoretically [11].

B. Antidot Lattices

A typical artificial lattice consists of arrays of antidots with circular repulsive potential. The system is characterized by the diameter d of an antidot and the period a. Such a lattice system is known to comprise with self-similar energy levels called Hofstadter's butterfly in magnetic fields [12], which are expected to give rise to intriguing electronic properties. The classical electron in the system is usually chaotic. Antidot lattices are one of such systems that the chaos plays important roles in their transport properties and a crossover between classical and quantum regimes can be realized.

Commensurability peaks were observed in the resistivity in weak magnetic fields $2R_c \approx a$ where R_c is the cyclotron radius [13]. In the limit of small aspect ratio $d/a \ll 1$, the electron loses its previous memory when it collides with an antidot and antidots are nothing but independent scatterers. In magnetic fields, the transport is possible through the migration of the center of the cyclotron motion. The scattering on an antidot cannot give rise to diffusion when $2R_c < a$ and starts to contribute to the conductivity when $2R_c > a - d$. The migration occurs most frequently due to successive scattering from nearest-neighbor antidots at the magnetic field $2R_c = a$ because the measure of such orbits becomes maximum in the phase space due to a magnetic focusing effect [14].

A fine oscillation was observed superimposed on commensurability peaks [15,16]. The period is roughly given by $\Delta B \sim \Phi_0/a^2$ with $\Phi_0 = ch/e$ being the magnetic flux quantum. This oscillation has been analyzed in terms of the periodic orbit theory giving a semiclassical quantization in chaotic system and has been shown to be closely related to quantized energy levels associated with a periodic orbit encircling a quantum dot.

C. Dot Arrays and Exotic Lattices

With the use of dot and antidot arrays, it is possible to fabricate 2D crystals with arbitrary structure. Some energy bands in a so-called Kagome lattice are known to be independent of the wave vector. Such flat-band systems can have a ferromagnetic ground state according to a known exact theorem. There has been a suggestion that ferromagnetism is realized in dot arrays if their parameters are appropriate [17]. A flat-band system can be realized in a finite-width honeycomb lattice giving rise to peculiar edge states [18]. The basic lattice structure of high-T_c cuprates is the 2D square lattice and a model system may be realized by dot arrays which exhibits superconductivity due to electron-electron interactions.

A honeycomb lattice is another interesting crystal exhibiting unique properties. A unit cell contains two carbon atoms denoted by A and B as shown in Fig. 1. Two bands having approximately a linear dispersion cross the Fermi level at K and K' points of the Brillouin zone. The effective-mass Hamiltonian for the K point is given by

$$\gamma(\boldsymbol{\sigma}\cdot\hat{\boldsymbol{k}})\boldsymbol{F}(\boldsymbol{r}) = \varepsilon\boldsymbol{F}(\boldsymbol{r}), \quad \boldsymbol{F}(\boldsymbol{r}) = \begin{pmatrix} F_A(\boldsymbol{r}) \\ F_B(\boldsymbol{r}) \end{pmatrix}, \qquad (3.1)$$

where $\boldsymbol{\sigma} = (\sigma_x, \sigma_y)$ is the Pauli spin matrix, γ is a band parameter, $\hat{\boldsymbol{k}} = -\mathrm{i}\boldsymbol{\nabla}$, and F_A and F_B represent the amplitude at two carbon sites A and B, respectively [19]. The above equation is same as Weyl's equation for a neutrino with vanishing rest mass and constant velocity independent of the wave vector. The energy becomes $\varepsilon_s(\boldsymbol{k}) = \pm\gamma|\boldsymbol{k}|$ The velocity is given by $|\boldsymbol{v}| = \gamma/\hbar$ independent of $\boldsymbol{k}$ and ε. The density of states becomes $D(\varepsilon) = |\varepsilon|/2\pi\gamma^2$. Figure 2 shows the energy dispersion

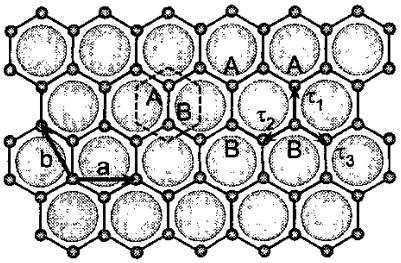

Figure 1: The structure of a honeycomb lattice. A unit cell contains two atoms denoted as A and B (small circles). It can be realized by fabrication of a short-period hexagonal antidot array (shadowed big circles).

and the density of states.

An important feature is the presence of a topological singularity at $\boldsymbol{k}=0$. A neutrino has a helicity and its spin is quantized into the direction of its motion. The spin eigen function changes its signature due to Berry's phase under a 2π rotation. Therefore the wave function acquires phase $-\pi$ when the wave vector $\boldsymbol{k}$ is rotated around the origin along a closed contour [20,21]. The signature change occurs only when the closed contour encircles the origin $\boldsymbol{k}=0$ but not when the contour does not contain $\boldsymbol{k}=0$. This topological singularity at $\boldsymbol{k}=0$ causes a zero-mode anomaly in the conductivity [22,23]. It gives rise to the absence of backscattering and perfect conductance in metallic carbon nanotubes.

IV. CARBON NANOTUBES

The electronic states of a carbon nanotube can be obtained by imposing periodic boundary conditions in the circumference direction except in extremely thin tubes, i.e., $\psi(\boldsymbol{r}+\boldsymbol{L})=\psi(\boldsymbol{r})$, where $\boldsymbol{L}$ is called the chiral vector and corresponds to the circumference of a nanotube. The angle η of $\boldsymbol{L}$ measured from the horizontal direction in Fig. 1 is called the chiral angle. Carbon nanotubes can be either a metal or semiconductor, depending on their diameters and helical arrangement. These conditions can be well reproduced in this $\boldsymbol{k}\cdot\boldsymbol{p}$ scheme [19].

In the $\boldsymbol{k}\cdot\boldsymbol{p}$ scheme, electrons in a nanotube can be regarded as neutrinos on a cylinder surface with a fictitious Aharonov-Bohm (AB) magnetic flux determined by $\boldsymbol{L}$. In metallic tubes, the flux vanishes and $\boldsymbol{F}$ satisfies periodic boundary conditions, while in semiconducting tubes, conditions for $\boldsymbol{F}$ include a nonzero AB phase. The scheme has been used successfully in the study of wide varieties of electronic properties. Some of such examples are magnetic properties [24] including the AB effect on the band gap, optical absorption spectra [25], exciton effects [26], lattice instabilities in the absence [27,28] and presence of a magnetic field [29], magnetic properties of ensembles of nanotubes [30], effects of spin-orbit interaction [31], junctions [32], vacancies [33], topological defects [34], and properties of nanotube caps [35].

The nontrivial Berry's phase leads to the unique property of a metallic nanotube that there exists no backscattering and the tube is a perfect conductor even in the presence of scatterers [21,36]. This has been demonstrated also by the conductance finite-length nanotubes

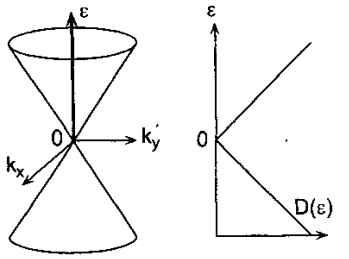

Figure 2: The energy dispersion and density of states in a honeycomb lattice.

containing many impurities [36] and by a tight binding calculation [37].

Backscattering corresponds to a rotation of the $\boldsymbol{k}$ direction by $\pm\pi$. In the absence of a magnetic field, there exists a time reversal process corresponding to each backscattering. This process involves a rotation by $\pm\pi$ in the opposite direction. The scattering amplitude of these two processes has an opposite signature because of Berry's phase and cancels out each other completely. In semiconducting nanotubes, on the other hand, backscattering appears because the symmetry is destroyed by a nonzero AB magnetic flux.

An important information has been obtained on the mean free path in nanotubes by single-electron tunneling experiments [38,39]. The Coulomb oscillation in semiconducting nanotubes is quite irregular and can be explained only if nanotubes are divided into many separate spatial regions in contrast to that in metallic nanotubes [40]. This behavior is consistent with the presence of backscattering leading to a localization of the wave function. In metallic nanotubes, the wave function is extended in the whole nanotube because of the absence of backscattering. With the use of electrostatic force microscopy the voltage drop in a metallic nanotube has been shown to be negligible [41].

At nonzero temperatures, lattice vibrations usually constitute the major source of electron scattering and limit the resistivity. Usually long-wavelength acoustic phonons, described by a continuum model [42], are most important. A phonon gives rise to a deformation potential $V_1 = g_1(u_{xx}+u_{yy})$ as a diagonal term, where $\boldsymbol{u}$ represent lattice displacements. It causes also a change in the distance between neighboring atoms, which gives rise to an off-diagonal term $V_2 = g_2 e^{3i\eta}(u_{xx}-u_{yy}+2iu_{xy})$

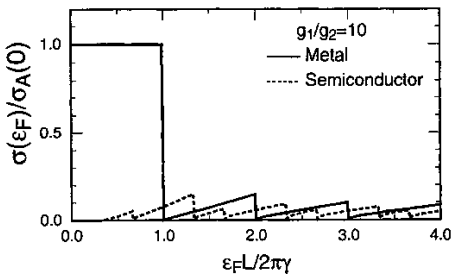

Figure 3: The Fermi-energy dependence of the conductivity for metallic (solid line) and semiconducting (broken line) nanotubes with $g_1/g_2=10$. $\sigma_A(0)$ is the conductivity at vanishing Fermi energy [43].

where g_2 is much smaller than g_1.

The diagonal term does not contribute to the backscattering as in the case of impurities and only the much smaller off-diagonal term has some contribution. The mean free path is estimated as $\sim 600L$ with $L = |\boldsymbol{L}|$ at room temperature, which is larger than 1 μm for thin armchair nanotubes with diameter $\sim$1.5 nm and increases in proportion to L with L. This shows that a metallic nanotube is ballistic even at room temperature. The situation changes dramatically when other bands start to be occupied. Figure 3 shows the Fermi energy dependence of the conductivity obtained by solving Boltzmann equation [43].

V. SUMMARY

In summary, a brief review has been given of recent investigation of transport properties of nanostructures from semiconductor quantum wires and dots to artificial crystals. By designing various artificial structures like honeycomb or other lattices, it is possible realize exotic electronic properties. Carbon nanotubes can be regarded as one of such typical examples.

ACKNOWLEDGMENTS

This work has been supported in part by Grants-in-Aid for COE (12CE2004 "Control of Electrons by Quantum Dot Structures and Its Application to Advanced Electronics") and Scientific Research from the Ministry of Education, Science and Culture, Japan.

REFERENCES

[1] B. J. van Wees, H. van Houten, C. W. J. Beenakker, J. G. Williamson, L. P. Kouwenhoven, D. van der Marel, and C.T. Foxon, Phys. Rev. Lett. **60** (1988) 848.

[2] H. van Houten, B.J. van Wees, J.E. Mooij, C.W.J. Beenakker, J.G. Williamson, and C.T. Foxon, Europhys. Lett. **5** (1988) 721.

[3] Y. Takagaki, K. Gamo, S. Namba, S. Ishida, S. Takaoka, K. Murase, K. Ishibashi, and Y. Aoyagi, Solid State Commun. **68** (1989) 1051.

[4] M. L. Roukes, A. Scherer, S. J. Allen, Jr., H. G. Craighead, R. M. Ruthen, E. D. Beebe, and J. P. Harbison, Phys. Rev. Lett. **59** (1987) 3011.

[5] L. J. Geerligs, V. F. Anderegg, P. A. M. Holweg, J. E. Mooij, H. Pothier, D. Esteve, C. Uribina, and M. H. Devoret, Phys. Rev. Lett. **64** (1990) 2691.

[6] S. Tarucha, D. G. Austing, T. Honda, R. J. van der Hage, and L. P. Kouwenhoven, Phys. Rev. Lett. **77** (1996) 3613.

[7] M. Pi, A. Emperador, M. Barranco, F. Garcias, K. Muraki, S. Tarucha, and D. G. Austing, Phys. Rev. Lett. **87** (2001) 66801.

[8] D. Goldhaber-Gordon, J. Gores, M. A. Kastner, H. Shtrikman, D. Mahalu, and U. Meirav, Phys. Rev. Lett. **81** (1998) 5225.

[9] R. R. Gerhardts, D. Weiss, and K. von Klitzing, Phys. Rev. Lett. **62** (1989) 1173.

[10] A. Messica, A. Soibel, U. Meirav, A. Stern, H. Shtrikman, V. Umansky, and D. Mahalu, Phys. Rev. Lett. **78** (1997) 705.

[11] S. Uryu and T. Ando, Phys. Rev. B **64** (2001) 195334.

[12] D. Hofstadter, Phys. Rev. B **14** (1976) 2239

[13] D. Weiss, M.L. Roukes, A. Menschig, P. Grambow, K. von Klitzing, and G. Weimann, Phys. Rev. Lett. **66** (1991) 2790.

[14] T. Ando, S. Uryu, and S. Ishizaka, Jpn. J. Appl. Phys. **38** (1999) 308.

[15] F. Nihey and K. Nakamura, Physica B **184** (1993) 398

[16] D. Weiss, K. Richter, A. Menschig, R. Bergmann, H. Schweizer, K. von Klitzing, and G. Weimann, Phys. Rev. Lett. **70** (1993) 4118

[17] H. Tamura, K. Shiraishi, and H. Takayanagi, Jpn. J. Appl. Phys. **39** (2000) L241.

[18] M. Fujita, K. Wakabayashi, K. Nakada and K. Kusakabe, J. Phys. Soc. Jpn. **65** (1996) 1920.

[19] H. Ajiki and T. Ando, J. Phys. Soc. Jpn. **62** (1993) 1255.

[20] M. V. Berry, Proc. Roy. Soc. London **A392** (1984) 45.

[21] T. Ando, T. Nakanishi, and R. Saito, J. Phys. Soc. Jpn. **67** (1998) 2857.

[22] N. H. Shon and T. Ando, J. Phys. Soc. Jpn. **67** (1998) 2421.

[23] T. Ando, Y. Zheng, and H. Suzuura, J. Phys. Soc. Jpn. **71** (2002) 1318-1324.

[24] H. Ajiki and T. Ando, J. Phys. Soc. Jpn. **62** (1993) 2470. [Errata, J. Phys. Soc. Jpn. **63** (1994) 4267.]

[25] H. Ajiki and T. Ando, Physica B **201** (1994) 349; Jpn. J. Appl. Phys. Suppl. **34-1** (1995) 107.

[26] T. Ando, J. Phys. Soc. Jpn. **66** (1997) 1066.

[27] N. A. Viet, H. Ajiki, and T. Ando, J. Phys. Soc. Jpn. **63** (1994) 3036.

[28] H. Suzuura and T. Ando, *Proc. 25th Int. Conf. Phys. Semicond.*, edited by N. Miura and T. Ando (Springer, Berlin, 2001), p. 1525.

[29] H. Ajiki and T. Ando, J. Phys. Soc. Jpn. **64** (1995) 260; **65** (1996) 2976.

[30] H. Ajiki and T. Ando, J. Phys. Soc. Jpn. **64** (1995) 4382.

[31] T. Ando, J. Phys. Soc. Jpn. **69** (2000) 1757.

[32] H. Matsumura and T. Ando, J. Phys. Soc. Jpn. **67** (1998) 3542;

[33] T. Ando, T. Nakanishi, and M. Igami, J. Phys. Soc. Jpn. **68** (1999) 3994.

[34] H. Matsumura and T. Ando, J. Phys. Soc. Jpn. **70** (2001) 2657.

[35] T. Yaguchi and T. Ando, J. Phys. Soc. Jpn. **70** (2001) 3641-3649; **71** (2002) No. 9.

[36] T. Ando and T. Nakanishi, J. Phys. Soc. Jpn. **67** (1998) 1704.

[37] T. Nakanishi and T. Ando, J. Phys. Soc. Jpn. **68** (1999) 561.

[38] S. J. Tans, M. H. Devoret, H. Dai, A. Thess, R. E. Smalley, L. J. Geerligs, and C. Dekker, Nature (London) **386** (1997) 474.

[39] A. Bezryadin, A. R. M. Verschueren, S. J. Tans, and C. Dekker, Phys. Rev. Lett. **80** (1998) 4036.

[40] P. L. McEuen, M. Bockrath, D. H. Cobden, Y. -G. Yoon, and S. G. Louie, Phys. Rev. Lett. **83** (1999) 5098.

[41] A. Bachtold, M. S. Fuhrer, S. Plyasunov, M. Forero, E. H. Anderson, A. Zettl, and P. L. McEuen, Phys. Rev. Lett. **84** (2000) 6082.

[42] H. Suzuura and T. Ando, Physica E **6** (2000) 864; Mol. Cryst. Liq. Cryst. **340** (2000) 731; Phys. Rev. B **65** (2002) 235412.

[43] H. Suzuura and T. Ando, Phys. Rev. B **65** (2002) 235412.